Model Predictive Multi-Objective Vehicular Adaptive Cruise Control

Shengbo Li, Keqiang Li, Rajesh Rajamani, and Jianqiang Wang

Abstract—This paper presents a novel vehicular adaptive cruise control (ACC) system that can comprehensively address issues of tracking capability, fuel economy and driver desired response. A hierarchical control architecture is utilized in which a lower controller compensates for nonlinear vehicle dynamics and enables tracking of desired acceleration. The upper controller is synthesized under the framework of model predictive control (MPC) theory. A quadratic cost function is developed that considers the contradictions between minimal tracking error, low fuel consumption and accordance with driver dynamic car-following characteristics while driver longitudinal ride comfort, driver permissible tracking range and rear-end safety are formulated as linear constraints. Employing a constraint softening method to avoid computing infeasibility, an optimal control law is numerically calculated using a quadratic programming algorithm. Detailed simulations with a heavy duty truck show that the developed ACC system provides significant benefits in terms of fuel economy and tracking capability while at the same time also satisfying driver desired car following characteristics.

Index Terms—Adaptive cruise control (ACC), driver characteristics, fuel economy, model predictive control (MPC), tracking capability.

I. INTRODUCTION

ADAPTIVE cruise control (ACC) is an enhancement of the traditional cruise control (CC) system that improves driver convenience, reduces driver workload and has the potential to improve vehicle safety. Current ACC systems that have been commercialized by automotive manufacturers focus entirely on the tasks of tracking a desired spacing from a preceding vehicle or tracking a desired speed. Researchers have recently started to explore the introduction of additional objectives into an ACC, e.g., fuel economy and driver desired response. Tsugawa [1] and Ioannou [2], [3] suggested the use of ITS technologies, including adaptive cruise control, to reduce fuel consumption of vehicles. Marsden *et al.* [4] considered issues of driver desired response and indicated the necessity to adapt to drivers' individual driving characteristics. While it would be beneficial to have an ACC that simultaneously considers issues of spacing control, fuel economy, and adaptability to individual driver characteristics, the design of the control system becomes a significant challenge when there are multiple objectives involved.

A review of current literature shows that an ACC that considers many objectives has not yet been developed. For CC systems with a given route, Latterman *et al.* [5] proposed an optimal control algorithm that minimizes the fuel consumption globally. Ioannou *et al.* [2], [3] pointed out that the smoothing feature of ACC vehicles could improve fuel efficiency of mixed traffic flow, including that of the ACC vehicle itself. Their research further disclosed that the effect was more obvious under conditions of large acceleration, lane changing and cut-in/off. On its basis, Zhang *et al.* [6] developed a nonlinear filter-based PI controller, which restricted acceleration levels to fulfill fuel-saving requirements. Similarly, Jonsson *et al.* [7] proposed a dynamic programming based offline control method. It reduced the fuel consumption while allowing more tracking error. With respect to driver desired response, ACC is usually designed to accord with three kinds of driver features: driver desired distance characteristic, driver longitudinal ride comfort and driver dynamic car-following characteristic. The first feature is normally embodied by integrating a driver desired clearance (DDC) model into the car-following system [5]–[13]. For the second feature, the vehicle acceleration and its derivative are typically restrained in order to avoid large acceleration and jerk [8], [9]. For the third feature, a common method is to integrate directly or indirectly a driver car-following (DCF) model into the ACC controller. For instance, Persson *et al.* [10] combined a linear DCF model and a PI method together to develop an upper layer controller for ACC. Using a second order inertial system as a reference model, Higashimata *et al.* [11] designed an ACC algorithm based on a model matching control structure to improve driver desired response in dynamic car-following scenarios.

However, the mentioned objectives such as tracking capability, fuel economy, and driver desired response usually conflict with each other. It is inadequate to design an ACC algorithm simply considering only one of them. The improvement of fuel consumption usually decreases the acceleration performance and lowers the tracking capability. This will lead to two problems consequently: 1) when the preceding car accelerates, larger inter-vehicular distance occurs due to the deficient acceleration performance, resulting in frequent vehicle cut-ins from adjacent lanes; 2) when the preceding vehicle decelerates, inter-vehicular distance shortens quickly and rear-end collisions happen more easily. On the contrary, if an ACC system pursues good tracking capability only, it leads to unnecessary acceleration and emergency braking, which also deteriorates the fuel economy of vehicles to an extent. Similarly, when drivers cannot adapt themselves to their ACC system, frequent driver

S. Li, K. Li, and J. Wang are with State Key Laboratory of Automotive Safety and Energy, Tsinghua University, Beijing 100084, P.R. China (e-mail: likq@tsinghua.edu.cn).

R. Rajamani is with the University of Minnesota, Minneapolis, MN 55455 USA (e-mail: rajamani@me.umn.edu).

intervention inevitably occurs. This action not only affects the improvement of tracking capability, but also deprives ACC of its benefit of reducing driver workload and enhancing vehicle safety. Therefore, it is necessary to comprehensively deal with all the three objectives simultaneously in one framework.

The design of an ACC system with multiple objectives can be naturally cast into a model predictive control (MPC) framework. MPC has already proved its merit in ACC design in literature, in spite of its considerable computational burden. However, the use of MPC has only been done to improve system performance in terms of tracking capability and to ensure proper transitions between different modes of operation. To ensure safety and good tracking capability, Corona *et al.* [12], [13] applied a Hybrid MPC approach to vehicular-following control. Kohut *et al.* [14] designed a predictive control strategy that optimizes the engine torque to tradeoff fuel consumption and trip time while keeping the vehicle within a specified speed envelope. For transitional maneuver modes, Bageshwar *et al.* [15] presented an MPC-based headway control algorithm with acceleration limitations incorporated explicitly to meet the requirements of ride comfort and safety.

Unlike the previous publications, the present paper focuses on the use of MPC to achieve multiple objectives during the vehicle-following mode in ACC. The multiple objectives sought to be achieved are desired driver response, minimal fuel consumption and minimization of car following error. In addition, hard and soft constraints that ensure vehicle safety and take actuator limits and ride quality into consideration are included in the problem formulation. This paper is organized as follows. In Section II, the lower layer controller is discussed under a hierarchical control structure and a three-state space model of the car-following system is built. In Section III, based on the framework of MPC, a predictive optimization problem is constructed considering tracking capability, fuel economy and driver desired response. In Section IV, a constraint softening method is adopted to address computing infeasibility issues and the optimal control law of MO-ACC is numerically solved. In Section IV, its success is demonstrated with a nonlinear high-order longitudinal model of a heavy duty (H/D) truck.

II. MODELING OF CAR-FOLLOWING SYSTEM

A. Nonlinearity Compensation of Vehicle Longitudinal Dynamics

The longitudinal dynamics of a vehicle are nonlinear. Its salient features include the static nonlinearity of engine torque maps, time varying gear position and aerodynamic drag force as a quadratic function of vehicle speed [16]. As in many other longitudinal vehicle control applications, we utilize a hierarchical controller consisting of a lower level controller and an upper level controller, as shown in Fig. 1.

The lower level controller determines the acceleration pedal position a_{accl} and brake pressure P_{brk} inputs so as to ensure that the desired acceleration $a_{f\mathrm{des}}$ is tracked by the actual acceleration a_f while the upper level controller determines the desired longitudinal acceleration according to inter-vehicle states and vehicle states. In Fig. 1, vehicle states, including engine
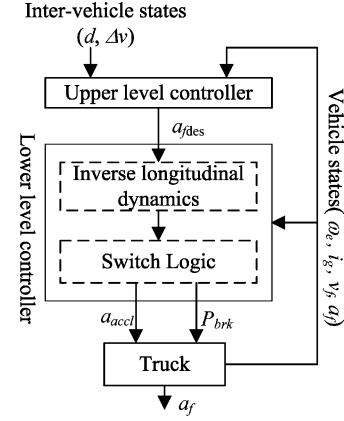

Fig. 1. Hierarchical control architecture.

speed ω_e, gear ratio i_g, vehicle speed v_f, and vehicle acceleration a_f, are measured by on-board sensors. Inter-vehicle states, including distance d and speed error Δv, are measured by radar equipped in the front of the ACC vehicle's engine cabin.

When synthesizing the lower level controller, one of the challenges is the presence of several nonlinearities coming from engine, transmission, and aerodynamic drag. To compensate them, we use the inverse dynamics control design method, as in [9]. A switching logic with a hysteresis boundary is adopted to avoid simultaneous actions from the drive train and braking system. Obviously, the lower layer controller which provides acceleration tracking and the truck together yield a new plant with its input $a_{f\mathrm{des}}$ and its output a_f, herein called generalized vehicle longitudinal dynamic (GVLD) system. Its input/output dynamics is described by a first-order system

$$a_f = \frac{K_L}{T_L s + 1} a_{f\mathrm{des}} \tag{1}$$

where K_L is the system gain and T_L is the time constant. Adopting a frequency response method introduced in [17], the parameters for the truck are identified as $K_L = 1.0$ and $T_L = 0.45$. When synthesizing the upper layer controller, it is assumed that the GVLD system is working effectively such that the dynamics of (1) is satisfied. This implies that the uncertainties caused by unmodeled power train dynamics, errors of vehicle parameters and external disturbances, e.g., road slope, are neglected during control design. However, while (1) is used as the assumption for designing the upper level controller, the actual simulations to be presented later in this paper use a high-order nonlinear longitudinal vehicle model that includes vehicle inertial and power train dynamics.

B. Three-State Space Model for Car-Following System

For the purpose of synthesizing the upper layer controller, we build the model of car-following system by integrating the GVLD system and an inter-vehicular longitudinal dynamics system. Fig. 2 shows its sketch.

With respect to inter-vehicular longitudinal dynamics, two state variables are defined: clearance error $\Delta d = d - d_{\mathrm{des}}$ and speed error $\Delta v = v_p - v_f$. The symbol v_p denotes the preceding
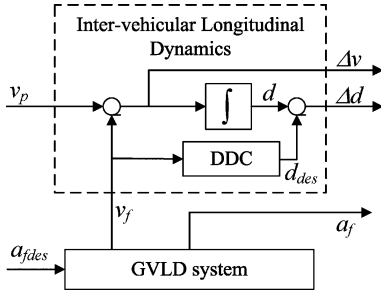
Fig. 2.   Sketch of car-following system.

vehicle's speed and d_{des} donates driver desired inter-vehicle distance. The d_{des} is typically calculated by a driver desired clearance (DDC) model. Here, we employ the constant time headway spacing policy [9] to describe it

$$d_{\text{des}} = \tau_h v_f + d_0 \qquad (2)$$

where $\tau_h = 2.5$ s is nominal time headway, $d_0 = 5$ m is the stopping distance for typical truck drivers. Note that the time-gap of $\tau_h = 2.5$ s is larger for truck drivers than for typical passenger car drivers. Considering inter-vehicular dynamics and (1) together, a three-state space model for car-following system is formulated as

$$
\begin{aligned}
\dot{x} &= \Phi x + \Pi u + \Gamma v \\
\Phi &= \begin{bmatrix} 0 & 1 & -\tau_h \\ 0 & 0 & -1 \\ 0 & 0 & -1/T_L \end{bmatrix} \\
\Pi &= \begin{bmatrix} 0 \\ 0 \\ K_L/T_L \end{bmatrix} \\
\Gamma &= \begin{bmatrix} 0 \\ 1 \\ 0 \end{bmatrix} \\
x &= \begin{bmatrix} \Delta d & \Delta v & a_f \end{bmatrix}^T \\
u &= a_{f\text{des}} \\
v &= a_p
\end{aligned}
\qquad (3)
$$

where a_p is the preceding vehicle's acceleration, $u \in R^1$ represents the control input, $v \in R^1$ represents the measurable disturbance and $x \in R^3$ represents the system state. Considering the fact that an MPC algorithm is usually designed and implemented in the discrete-time domain, the continuous-time (3) is converted into a discrete-time model by zero-order hold (ZOH) discretization, yielding

$$x(k+1) = Ax(k) + Bu(k) + Gv(k) \qquad (4)$$

where k represent the kth sampling point, A, B, and G are system matrices, mathematically expressed as

$$A = \sum_{k=0}^{\infty} \frac{\Phi^k T_s^k}{k!}$$

$$
\begin{aligned}
B &= \sum_{k=0}^{\infty} \frac{\Phi^{k-1} T_s^k}{k!} \Pi \\
G &= \sum_{k=0}^{\infty} \frac{\Phi^{k-1} T_s^k}{k!} \Gamma
\end{aligned}
\qquad (5)
$$

where $T_s = 100$ ms is sampling time. For a typical ACC vehicle equipped with both radar and accelerometer, all of the states in (4) are measurable, giving the output equation

$$y(k) = Cx(k), C = \begin{bmatrix} 1 & 0 & 0 \\ 0 & 1 & 0 \\ 0 & 0 & 1 \end{bmatrix} \qquad (6)$$

where C is an identity matrix and $y \in R^3$ is the measurement of system state.

III. Construction of Predictivve Optimization Problem

Tracking capability, fuel economy, driver desired response, safety and environmental issues, as well as limitations from vehicles and traffic flow—all of these shape the behavior of an ACC system. In MO-ACC, great emphasis is given to the former three terms, namely, necessary tracking capability, high fuel economy and good driver desired response.

For the purpose of quantifying them, we refine the definition of the three objectives. The first objective is divided into the following three parts:

(A1)   when the preceding vehicle is at steady state, the tracking errors should converge to small values;

(A2)   when the preceding vehicle accelerates, the inter-vehicle states should satisfy a driver permissible tracking range as much as possible to avoid frequent preceding vehicles' cut-in from adjacent lanes;

(A3)   when the preceding vehicle decelerates, rear-end collision must be avoided.

The second objective is to (B1) reduce the fuel consumption when ACC is activated. With respect to the third objective, the following three kinds of driver characteristics should be satisfied:

(C1)   driver desired distance characteristic;

(C2)   driver longitudinal ride comfort;

(C3)   driver desired dynamic car-following characteristic.

In those sub-objectives, sub-objective (C1) has been realized in the form of DDC model in (3). The others are collected into two groups in order to quantify them under the MPC framework. The sub-objectives (A1) (B1) and (C3) are quantified to be 2-norm cost functions and (A2), (A3), (C2) are formulated as linear constraints. They together yield a tractable model predictive optimization problem.

It should be noted that although tracking capability is somewhat sacrificed in the MO-ACC in order to achieve fuel economy, satisfaction of the three sub-objectives A1, A2, and A3 described above ensures the safety of the vehicle and driver-acceptable tracking performance.

A. Cost Function Design in Predictive Optimization Problem

The tracking capability is usually specified in terms of speed error and distance error. In order to quantitatively describe (A1),

a 1-norm function of tracking errors is adopted as the cost function of MPC in [12] and a 2-norm function is used in [15]. The former gives equal consideration to the tracking errors of different degrees while the latter tends to penalize larger errors and neglect smaller ones. Actually, in a car-following process, a driver only responds to large enough tracking errors and isn't sensitive to tiny ones. This means the driver maintains a constant pedal position when the tracking errors are in the range of specific thresholds. This feature is called Action Point [18]. Only when the errors exceed the Action Point, the driver will then adjust throttle pedal or brake pedal to bring tracking errors back into the range of Action Point. This helps reduce fuel consumption, since the driver doesn't frequently accelerate or decelerate under small-tracking errors. Therefore, from the viewpoint of the driver, it is more reasonable to employ the 2-norm of tracking errors to quantify (A1)

$$L_{TE} = w_{y\Delta v}\Delta v^2 + w_{y\Delta d}\Delta d^2 \tag{7}$$

where $w_{y\Delta v}$ and $w_{y\Delta d}$ are the corresponding weighting coefficients.

A direct method to quantify the sub-objective (B2) is to include the fuel injection amount of engine as a variable in the cost function. However, this has a nonlinear relationship with the system states in (3). Such a cost function will definitely lead to a nonlinear programming problem in MPC. Its large computing complexity makes its difficult to be solved in a sampling time less than $T_s = 100$ ms. As mentioned in [1] and [6], fuel consumption is mainly dominated by vehicle acceleration levels if neglecting extremes in engine operational area. In a car-following process with same mileage and average travel speed, fuel consumption of a vehicle increases as the absolute of its acceleration increases. Regarding the fuel economy of vehicles, the penalty for vehicle acceleration has a similar effect as that of a penalty directly on the fuel consumption, but resulting in a QP rather than a nonlinear program. Here, considering that the input and output of GVLD system are similar to each other, the sub-objective (B2) is defined as a 2-norm function of desired longitudinal acceleration and its derivative instead of actual longitudinal acceleration and jerk

$$L_{FC} = w_u a_{f\text{des}}^2 + w_{du} \dot{a}_{f\text{des}}^2 \tag{8}$$

where w_u is the weighting coefficient of $a_{f\text{des}}$, w_{du} is that of $\dot{a}_{f\text{des}}$. In (8), the second term in the right-hand side can not only restrain frequent variation of engine speed by reducing the longitudinal jerk, but also helps to improve longitudinal ride comfort of passengers.

In the car-following process during a transient maneuver, the tracking errors are not zero. The driver normally manipulates the acceleration pedal or brake pedal to make the vehicle track the driver's desired reference trajectory. Here, the trajectory is calculated by a DCF model. The tracking errors between system output and reference trajectory is minimized to embody the sub-objective (C3). Therefore, its quantification is a 2-norm of the error between actual acceleration and reference acceleration

$$L_{DC} = w_{ya}(a_{fR} - a_f)^2 \tag{9}$$

where w_{ya} is the weighting coefficient and a_{fR} is the reference acceleration calculated by a linear DCF model

$$a_{fR} = k_V \cdot \Delta v + k_D \cdot \Delta d \tag{10}$$

where $k_V = 0.25$ and $k_D = 0.02$ are parameters for typical H/D truck drivers. The experimental data used to analyze driver behavior was obtained from both city road and high way in Kanagawa, Japan. Three professional truck drivers were involved, with 4 h of data recorded per driver. The model parameters are identified using a gradient search method. The fundamental idea is to search for the optimal parameters, which can minimize a quadratic cost function of errors between outputs of DCF model and driver experiment data in terms of longitudinal acceleration, relative speed and distance error. The detailed algorithm is described in [19]. In order to verify the precision of the linear DCF model (10), one section of experimental data is presented to compare acceleration, speed and distance between model and experiment. The figures for the comparison are shown in Fig. 3(a)–(c).

B. I/O Constraints in MPC Optimization Problem

For the ride comfort issue in ACC, paper [8] provides a criterion: 1) the vehicle acceleration is constrained; 2) the absolute value of jerk should be as small as possible. Here, we restrict both the acceleration and jerk to improve driver's longitudinal ride comfort. Considering that both the input and output of GVLD system are related to acceleration, we use the following linear equalities for sub-objective (C2):

$$\begin{aligned} a_{f\min} &< a_f < a_{f\max} \\ a_{f\min} &< a_{f\text{des}} < a_{f\max} \\ j_{f\min} &< \dot{a}_{f\text{des}} < j_{f\max} \end{aligned} \tag{11}$$

where $a_{f\min}, a_{f\max}$ are chosen as -1.5 m/s^2 and 0.6 m/s^2. The absolute of $a_{f\min}$ being bigger than that of $a_{f\max}$ can accommodate larger braking degree to prevent rear-end collision. Similarly, the absolute of $j_{f\min} = -1$ m/s^3 is selected to be bigger than that of $j_{f\max} = 0.1$ m/s^3. Note that these values provide for a change in acceleration of 1 m/s^2 in 10 s while allowing for a 10 times faster change in deceleration during braking.

When the preceding car runs uniformly, the minimization of (7) can guarantee convergent tracking errors. However, in MO-ACC with its priority on good fuel economy, the weighting coefficients of tracking errors are usually relatively small, leading to low tracking performance. A consequent problem is that when the preceding vehicle accelerates or decelerates, larger or smaller inter-vehicle distance may occur easily. Frequent cut-ins from adjacent lanes and driver's intervention on ACC may be induced due to larger inter-vehicle distance and unacceptable shorter inter-vehicle distances. In order to avoid the issue, a driver permissible tracking range criterion is employed to restrain Δd and Δv inside specific ranges. The inequalities for sub-objective (A2) are

$$\begin{aligned} \Delta d_{\min} &\leq \Delta d \leq \Delta d_{\max} \\ \Delta v_{\min} &\leq \Delta v \leq \Delta v_{\max} \end{aligned} \tag{12}$$
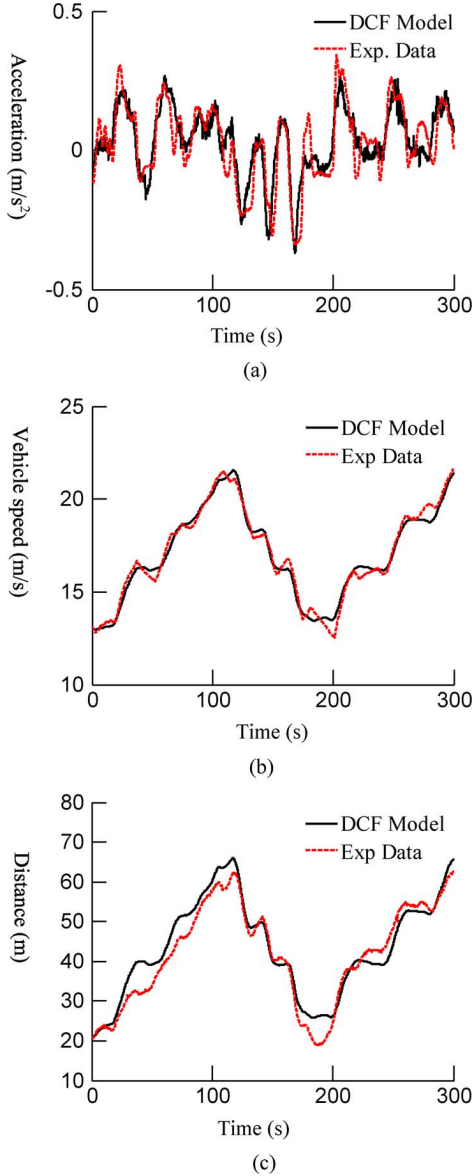
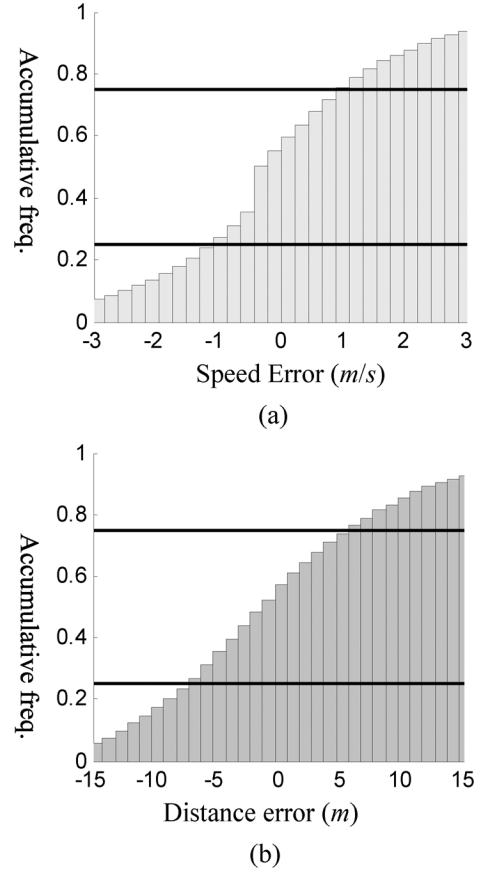Fig. 3. Comparison of experiment data and DCF model. (a) Acceleration. (b) Vehicle speed. (c) Distance.

Fig. 4. Identification of driver permissible tracking range. (a) Accumulative frequency of speed error. (b) Accumulative frequency of distance error.

where $\Delta d_{\min} = -5$ m is the lower boundary of Δd, $\Delta d_{\max} = 6$ m is the upper boundary of Δd, $\Delta v_{\min} = -1.0$ m/s is the lower boundary of Δv and $\Delta v_{\max} = 0.9$ m/s is the upper boundary of Δv. These values are again obtained from the driver experimental data described in Section III-A. The identification method is as follows.

The Δv and Δd data points in driver experiments in car-following conditions are accumulated, obtaining their accumulated distribution figures of Δv and Δd, as shown in Fig. 4. Two solid lines in each figure, mathematically expressed as unilateral frequency 25%, are shown to reflect driver acceptable upper and lower boundaries. The distance and speed error values located inside these boundaries are identified as driver permissible tracking error range.

The last sub-objective (A3) in MO-ACC is to avoid rear-end collisions, whenever physically possible. This translates into keeping a positive inter-vehicle distance. In [12], a minimum safety distance strategy is adopted to maintain car-following safety by forcing inter-vehicle distance to be larger than a constant value d_{s0}. Actually, safety distance is not constant, but related to vehicle speed. An example is when the preceding vehicle's speed is much smaller than that of the following one, an inter-vehicular distance larger than d_{s0} can be still dangerous. In [20], a time-to-collision (TTC) strategy is used to describe the relationship between safety distance and speed error in designing a forward collision warning system. Integrating the TTC strategy and the minimum safe distance strategy, we specify an inequality for rear-end safety as

$$d \geq d_s$$
$$d_s = \max\{\text{TTC} \cdot \Delta v, d_{s0}\} \tag{13}$$

where d_s is safe distance, $\text{TTC} = -3$ s is TTC value, $d_{s0} = 5$ m is minimum safe distance.

C. Model Predictive Optimization Problem for MO-ACC

In order to obtain a tractable predictive optimization problem, the three cost functions (7), (8) and (9) are combined together by employing a linear weighting method introduced in [21]. Then, discretizing the combined cost function with sampling time T_s

and resettling in finite predictive horizon $P \cdot T_s$, it yields the cost function to be optimized

$$
\begin{aligned}
L(y, u, \Delta u) = &\sum_{i=0}^{p-1} \|\Omega y(k+i+1|k)\|_{w_y}^2 \\
&+ \sum_{i=0}^{p-1} \|u(k+i|k)\|_{w_u}^2 \\
&+ \sum_{i=0}^{p-1} \|\Delta u(k+i|k)\|_{w_{\Delta u}}^2
\end{aligned}
\tag{14}
$$

where $\Delta u(\mathrm{k}) = u(k) - u(k-1)$ is the control increment, P is the length of predictive horizon, $(k+i \,|\, k)$ denotes the predicted value at time $k + i$ based on the information at time k, w_y is weighting matrix of system output, w_u is that of control input, $w_{\Delta u}$ is that of control increment, Ω is a transforming matrix related to the DCF model. They are expressed as

$$
\Omega = \begin{bmatrix} -1 & 0 & 0 \\ 0 & -1 & 0 \\ k_D & k_V & -1 \end{bmatrix}, \quad w_{\Delta u} = \frac{w_{du}}{T_s^2}
$$

$$
w_y = \begin{bmatrix} w_{y\Delta d} & 0 & 0 \\ 0 & w_{y\Delta v} & 0 \\ 0 & 0 & w_{ya} \end{bmatrix}.
\tag{15}
$$

In order to obtain the I/O constraints for the predictive optimization problem, we rewrite the inequalities related to the control input u and its increment Δu in the predictive horizon

$$
\begin{aligned}
u_{\min} \le u(k+i|k) \le u_{\max} \\
\Delta u_{\min} \le \Delta u(k+i|k) \le \Delta u_{\max}
\end{aligned}, i = 0 : P - 1
\tag{16}
$$

where $u_{\min} = a_{f\min}$ is the lower boundary of $u, u_{\max} = a_{f\max}$ is the upper boundary of $u \Delta u_{\min} = j_{f\min} \cdot T_s$ is the lower boundary of $\Delta u, \Delta u_{\max} = j_{f\max} \cdot T_s$ is the upper boundary of Δu. Similarly, we rewrite the inequalities related to the system output y

$$
y_{\min} \le y(k+i+1 \,|\, k) \le y_{\max}, i = 0 : P - 1
\tag{17}
$$

where $y_{\min} = [\Delta d_{\min}, \Delta v_{\min}, a_{f\min}]^{\mathrm{T}}$ is the lower boundary of $y, y_{\max} = [\Delta d_{\max}, \Delta v_{\max}, a_{f\max}]^{\mathrm{T}}$ is the upper boundary of y. Integrating (2) and the definitions of $\Delta d, \Delta v$, the inequality for rear-end safety can be rewritten as

$$
a_{\mathrm{safe}} \cdot y(k+i+1 \,|\, k) \ge d_{\mathrm{safe}} + \tau_{\mathrm{safe}} v(k+i+1 \,|\, k)
\qquad i = 0 : P - 1
\tag{18}
$$

where $a_{\mathrm{safe}}, d_{\mathrm{safe}}$, and τ_{safe} are the coefficients, mathematically expressed as

$$
a_{\mathrm{safe}} = \begin{bmatrix} 1 & -\mathrm{TTC} - \tau_h & 0 \\ 1 & -\tau_h & 0 \\ 0 & 0 & 0 \end{bmatrix}
$$

$$
d_{\mathrm{safe}} = \begin{bmatrix} -d_0 \\ d_{S0} - d_0 \\ 0 \end{bmatrix},
$$

$$
\tau_{\mathrm{safe}} = \begin{bmatrix} -\tau_h \\ -\tau_h \\ 0 \end{bmatrix}.
\tag{19}
$$

The problem statement for the upper layer control algorithm of MO-ACC is to minimize the cost function (14) subject to the I/O constraints (16)–(18), and the model of the car-following system (4) and (6)

$$
\min_{\Delta u(k+i|k), i=0:P-1} L(y, u, \Delta u)
$$

Subj. to:

    (1) I/O constraints: (16), (17), and (18).

    (2) Model of car-following

    system: (4) and (6). $\tag{20}$

IV. RECEDING HORIZON CONTROL OF MO-ACC

A. Addressing Computing Infeasibility in MO-ACC Algorithm

A key issue with the MO-ACC algorithm is the computing infeasibility of the predictive optimization problem. One of the representative causes is that the tracking errors exceed the boundaries of hard constraints because of rapid acceleration/deceleration of the preceding vehicle. In such a situation, the problem (20) may have no optimal solution because the hard constraints in (16) and (17) are never satisfied. In order to solve it, we improve the problem (20) by employing a constraint softening method whose fundamental idea is to relax the I/O constraints so that they can be violated [22].

First, define a new cost function with an additional quadratic term of a slack variable

$$
\psi(y, u, \Delta u, \varepsilon) = L(y, u, \Delta u) + \rho \varepsilon^2
\tag{21}
$$

where ε is called the slack variable and ρ is its weighting coefficient. Then, the I/O constraints (16) and (17) are correspondingly transformed into softened constraints with a slack variable

$$
\begin{aligned}
\Delta u_{\min} + \varepsilon v_{\min}^{\Delta u} \le \Delta u(k+i \,|\, k) \le \Delta u_{\max} + \varepsilon v_{\max}^{\Delta u} \\
u_{\min} + \varepsilon v_{\min}^{u} \le u(k+i \,|\, k) \le u_{\max} + \varepsilon v_{\max}^{u} \\
y_{\min} + \varepsilon v_{\min}^{y} \le y(k+i+1 \,|\, k) \le y_{\max} + \varepsilon v_{\max}^{y} \\
\varepsilon \ge 0 \\
i = 0, \ldots, P - 1
\end{aligned}
\tag{22}
$$

where $v_{\min}^{\Delta u}, v_{\max}^{\Delta u}$ are called equal concerns for relaxation (ECR) of $\Delta u, v_{\min}^{u}, v_{\max}^{u}$ are ECRs of $u, v_{\min}^{y}, v_{\max}^{y}$ are ECR of y. Therefore, we have a predictive optimization problem modified by constraint softening method

$$
\min_{\varepsilon, \Delta u(k+i \,|\, k), i=0:P-1} \psi(y, u, \Delta u, \varepsilon)
$$

Subj. to:

    (1) I/O constraints:

    Softening constraint (22)

    and rear-end safety constraint (18).

    (2) Model of car-following

    system: (4) and (6). $\tag{23}$

TABLE I
PARAMETERS OF MO-ACC CONTROLLER

Para.	Value	Para.	Value
w_y	diag([0.06, 0.1, 0.5])	w_u	1.0
ρ	3	$w_{\Delta u}$	0.1
T_s	100 ms	--	--
$y_{\min}$	$[-5,-1,-1.5]^{\mathrm{T}}$	$y_{\max}$	$[6, 0.9, 0.6]^{\mathrm{T}}$
$u_{\min}$	-1.5	$u_{\max}$	0.6
$\Delta u_{\min}$	-0.1	$\Delta u_{\max}$	0.01
$v^y_{\min}$	$[-3,-1,-0.1]^{\mathrm{T}}$	$v^y_{\max}$	$[3, 1, 0.1]^{\mathrm{T}}$
$v^u_{\min}$	-0.1	$v^u_{\max}$	0.01
$v^{\Delta u}_{\min}$	0	$v^{\Delta u}_{\max}$	0
k_V	0.25	k_D	0.02
TTC	-3	d_{s0}	5

Fig. 5. Longitudinal dynamics of H/D truck.

In MO-ACC, when the hard boundaries of y, u, or Δu are exceeded, the slack variable ε will automatically become a positive value to allow violation of hard constraints, thus avoiding the potential computing infeasibility. Moreover, the violation degree is penalized by the quadratic term of ε in the cost function. It guarantees that preferable control optimality of MPC algorithm is still maintained. When the hard boundaries of y, u, or Δu are not exceeded, the hard constraints will not be violated and slack variable becomes zero. The optimization problem (23) degenerates into its standard form (20).

Additionally, the constraint from rear-end safety is not softened because rear-end collision is not allowable. Moreover, since constraints on Δu and u are capable of being violated, MO-ACC can increase ε and consequently strengthen the braking input when rear-end safety constraint is being exceeded. This helps avoid rear-end collisions as far as physically possible.

B. Numerical Computation of MO-ACC Control Law

The optimization problem (23) is transformed to a standard quadratic programming (QP) problem, and then solved by a Dantzig–Wolfe active set algorithm in each sampling time, thus obtaining the optimal control sequence $[\Delta u^*(k+i|k)]_{i=1:P}$ and the optimal slack variable ε^*. See [22] for detailed procedures. Considering the relationship between the input increment and the control input, we have the control law of MO-ACC as

$$u(k) = u(k-1) + \Delta u^*(k+0|k). \qquad (24)$$

Note: When solving the problem (23), the acceleration of preceding vehicle in predictive horizon must be known. Here, it is actually a recursion of $a_p(k)$ at current step. Descriptions of how the $a_p(k)$ can be estimated using a Kalman filter can be found in [23].

Key parameters in the MO-ACC algorithm are listed in Table I.

V. SIMULATIONS AND ANALYSIS

The goal of the following simulations is to evaluate the performance of the MO-ACC algorithm. These simulations are carried out with a nonlinear high-order H/D truck longitudinal model, whose schematic diagram is shown in Fig. 5. In Fig. 5, Q_{inj} is the fuel injection amount per cylinder in each stoke, T_e is the engine torque, i_g is the gear position, T_c is the clutch torque output, ω_c is the output speed of clutch, T_w is the driving force
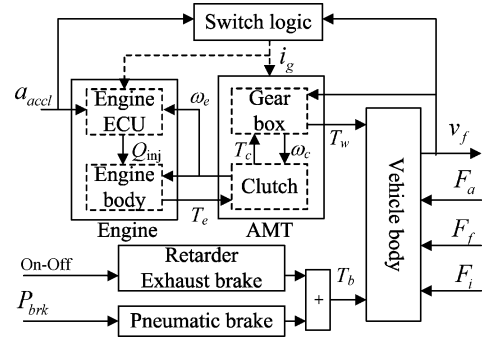
acting on tyres, T_b is the braking force acting on tyres, F_a is the aerodynamic drag, F_f is the rolling resistance, and F_i is the climbing resistance.

Here, the diesel engine is divided into engine ECU and engine body. The ECU is expressed as a complex lookup table with its inputs being $a_{\mathrm{accl}}, \omega_e$ and i_g, etc. The engine body is mainly described by a nonlinear function with it arguments as Q_{inj} and ω_e and its dynamics due to intake and combustion process is approximated by a first-order inertial system. It is assumed that the clutch has two modes: engagement and disengagement, of which the former is modeled as a second-order inertial system. The mechanical characteristics of AMT, final gear and the differential are all assumed as static functions. Pneumatic brake system is simplified to be a first order system with pure time delay. In the following simulation, it is assumed that both the retarder and engine brake are off. Vehicle body is described by a power balance equation between its traction/braking force and external resistance such as aerodynamic drag, rolling resistance, and climbing force.

For comparison of performance, a LQR-based ACC algorithm (LQACC) is also designed based on the same control plant (4). Like the ride comfort consideration in MO-ACC, its control law is also restrained by longitudinal ride comfort criterion. The weighting matrices of its cost function are identical to that of MO-ACC, that is $w_y = \mathrm{diag}([0.06, 0.1, 0.5])$ and $w_u = 1.0$. The LQACC control law is

$$u(k) = \begin{cases} a_{f\max}, & K \cdot y(k) > a_{f\max} \\ K \cdot y(k), & \text{otherwise} \\ a_{f\min}, & K \cdot y(k) < a_{f\min} \end{cases} \qquad (25)$$

where K is the control gain calculated by the LQR method. In order to demonstrate the special performance of MO-ACC algorithm, the simulation is tested under four kinds of traffic scenarios: Preceding car's rapid accelerating scenario, preceding car's emergency braking scenario, preceding car's normal accelerating scenario, and city road/highway driving cycles. The MO-ACC algorithm will be regarded successful if its application can improve both fuel economy and tracking capability while also meeting driver desired response and avoiding collisions.

A. Preceding Car's Rapid Acceleration Scenario

In the preceding car's rapid acceleration scenario, it is assumed that the ACC truck and preceding car run at the same
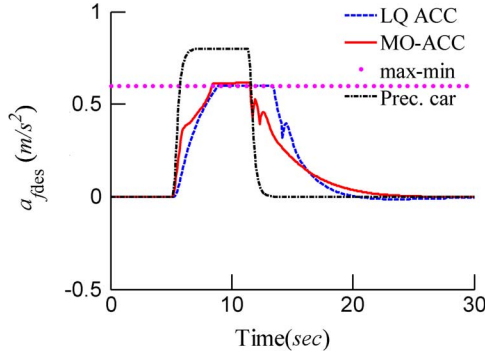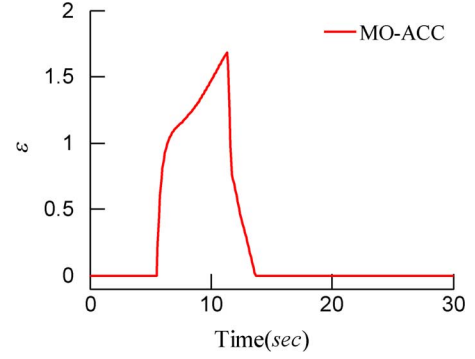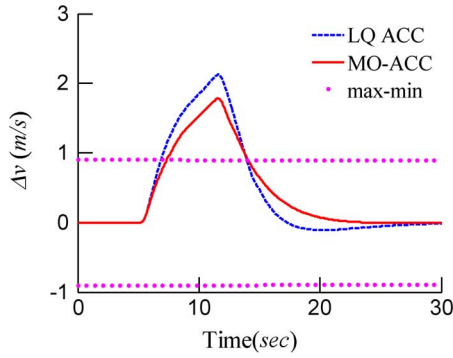
Fig. 6. Desired acceleration.

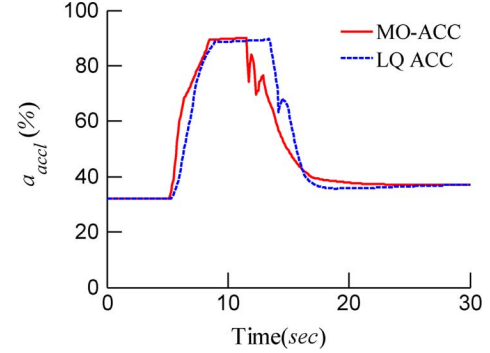Fig. 7. Speed error.

Fig. 8. Distance error.
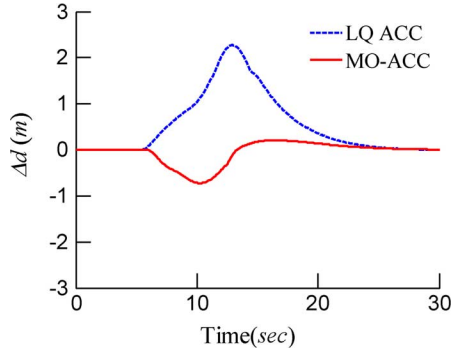

Fig. 9. Slack variable ε.

Fig. 10. Acceleration pedal.

initial speed. At 5 s, the preceding car accelerates at 0.8 m/s² from 10 to 15 m/s. The ACC truck is controlled to follow it by using the MO-ACC and LQACC algorithms, respectively. The results are shown in Figs. 6–11.

It is found from Fig. 6 that the desired acceleration under MO-ACC is between $a_{f\max}$ and $a_{f\min}$, satisfying the driver longitudinal ride comfort. From Figs. 7 and 8, it can be seen that even though the tracking errors exceed driver permissible range, MO-ACC avoids the computing infeasibility due to the introduction of slack variable ε into the hard constraints. When actual tracking errors exceed the boundaries of output constraints, the MO-ACC algorithm automatically increases ε to satisfy the boundary of inequality, shown as Fig. 9. Compared with LQACC, the time that the acceleration pedal input is large is shorter under MO-ACC, leading to lower acceleration levels. Moreover, due to the introduction of driver permissible tracking

range into I/O constraints, the tracking errors exceeding its boundaries are limited. As shown from Fig. 7, the maximum of Δv under MO-ACC is smaller than that under LQACC. So, both better fuel economy and better tracking capability can be foreseen in MO-ACC. When the tracking errors enter driver permissible range, ε becomes zero, giving no relaxation to the hard constraints. After the preceding car goes back to uniform speed, the MO-ACC can manipulate Δd and Δv into zero which indicates it is locally stable.

B. Preceding Car's Emergency Braking Scenario

In preceding car's emergency braking scenario, the preceding car decelerates at the acceleration of -2.5 m/s² from 15 to 1 m/s. The ACC truck is controlled to follow it by the MO-ACC and LQACC algorithms, respectively. The results are shown in Figs. 12 and 13.

From Figs. 12 and 13, it is found that due to the constraints coming from driver longitudinal ride comfort, the LQACC cannot provide enough braking force. The inter-vehicular distance reaches the safety boundary. And a rear end collision is possible if the preceding vehicle brakes more urgently. In contrast, as shown in Fig. 14, the MO-ACC can automatically increase the slack variable ε to strengthen the braking input when the actual distance approaches the safety boundary. It effectively reduces the possibility of rear-end collision.

C. Preceding Vehicle's Normal Acceleration Scenario

In the preceding vehicle's normal acceleration scenario, it is assumed that the ACC truck runs at the speed of 10 m/s with a preceding car ahead of it. At 5 s, the preceding car accelerates
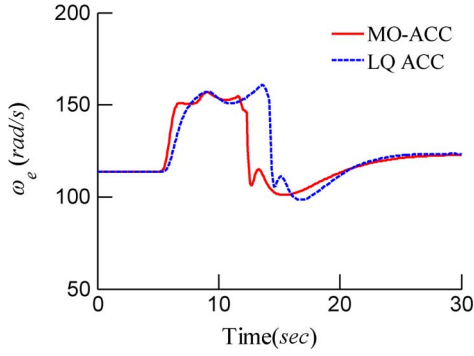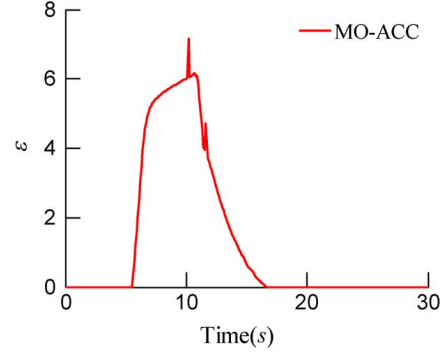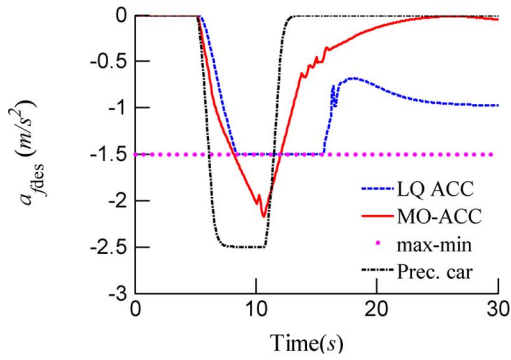
Fig. 11. Engine speed.

Fig. 12. Desired acceleration.
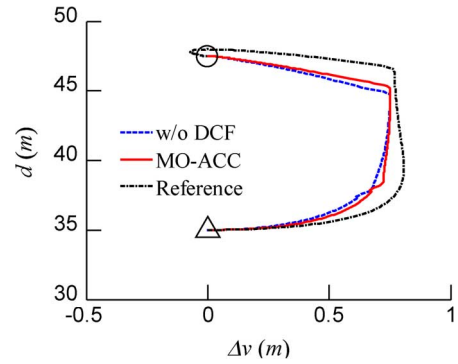

Fig. 13. Inter-vehicle distance.

Fig. 14. Slack variable ε.

Fig. 15. Phase plot of distance versus speed error.
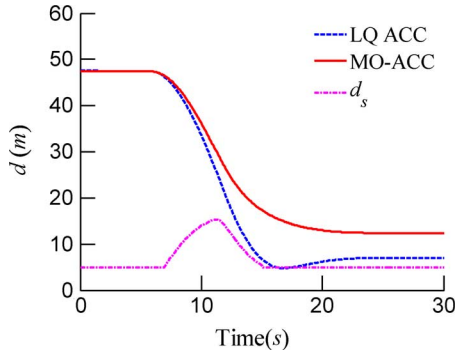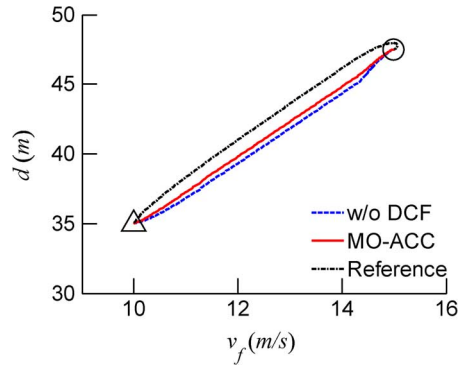

Fig. 16. Phase plot of distance versus vehicle speed.

at 0.3 m/s^2 from 10 to 15 m/s. Different from Sections V-A and V-B, the ACC truck is controlled by MO-ACC with DCF model and MO-ACC without DCF model in order to demonstrate the effectiveness of integrating the driver car-following model (10) into MO-ACC. Figs. 15 and 16 show the phase plot of $d - \Delta v$ and $d - v_f$, respectively, in which the triangle point is the starting point and the circle point is the stopping point.

In Figs. 15 and 16, the reference trajectory, shown as dotted-dashed line, is calculated from the DCF model, representing driver desired response for the car-following process. Compared with MO-ACC without DCF model, it is found that phase trajectory under MO-ACC is closer to reference trajectory, meaning

MO-ACC accords with dynamic car-following characteristics more. It means that the integration of DCF model is helpful in enabling driver desired dynamic car-following characteristics in the ACC algorithm.

D. City Road and Highway Driving Cycles

In order to verify the control performance comprehensively, driving cycles for city road and highway are adopted here. Their speed profiles are illustrated by the solid line and the dashed line in Fig. 17, respectively. Similar to Sections V-A and V-B,
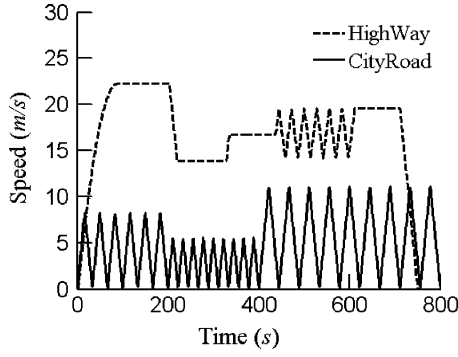
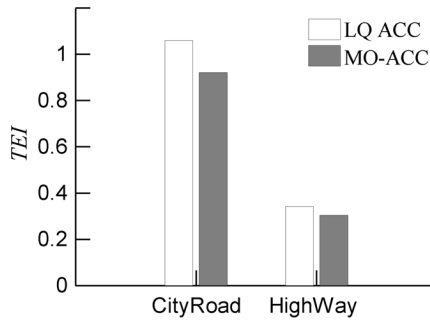Fig. 17. City road and highway driving cycles.

Fig. 18. Comparison in tracking capability.

the ACC truck is controlled to follow it by the MO-ACC and LQACC algorithms, respectively.

To comprehensively reflect tracking capability, define tracking error index (TEI) composed of both speed error and distance error as

$$\text{TEI} = \frac{1}{N} \sum_{k=1}^{N} \left(\left| \frac{\Delta d(k)}{K_{DV}} \right| + |\Delta v(k)| \right) \qquad (26)$$

where N is length of driving cycle, K_{DV} is weighting coefficient, reflecting different emphasis on Δd and Δv. Here, K_{DV} is selected as 10. The TEI values under city road and high way driving cycles are shown in Fig. 18. Its corresponding average fuel consumption per hundred kilometers (FCHM) is shown in Fig. 19. It is found that compared with the LQACC, both tracking capability and fuel consumption in the MO-ACC are improved. In the city road driving cycle, the TEI value is reduced by 14.8% while the FCHM value decreases by 5.9%. In the highway driving cycle, they are reduced by 11.5% and 2.2%, respectively.

VI. CONCLUSION

In this paper, model predictive control theory was employed to synthesize a MO-ACC algorithm in order to satisfy such control objectives as effective tracking capability, high fuel economy, driver desired response and collision avoidance simultaneously. The following is concluded.

1) Due to input constraints in MO-ACC, the vehicle acceleration can be limited to a specific range, thus ensuring driver longitudinal ride comfort and improving fuel economy.
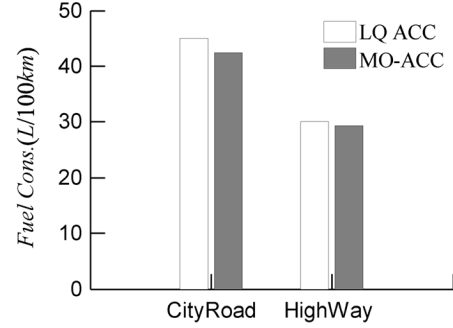

Fig. 19. Comparison in fuel economy.

2) The introduction of driver permissible tracking range helps to avoid cut-ins from other cars or unnecessary driver intervention due to uncomfortably larger or smaller inter-vehicle distances.

3) A constraint softening method avoids the computing infeasibility caused by hard I/O constraints. Together with output constraints resulting from rear-end safety considerations, this can strengthen the braking input when the actual inter-vehicle distance approaches the safety boundary, reducing the possibility of rear-end collision.

4) The integration of driver car-following model into the optimization problem enables driver desired dynamic car-following characteristics.

5) It has been clearly demonstrated that the MO-ACC controller can reduce fuel consumption of the ACC vehicle while not sacrificing the tracking or safety performance compared with the LQACC controller.

REFERENCES

[1] S. Tsugawa, "An overview on energy conservation in automobile traffic and transportation with ITS," in *Proc. IEEE Int. Veh. Elect. Conf.*, Japan, 2001, pp. 137–142.

[2] P. Ioannou and M. Stefanovic, "Evaluation of the ACC vehicles in mixed traffic: Lane change effects and sensitivity analysis," *IEEE Trans. Intel. Transport. Syst.*, vol. 6, no. 1, pp. 79–90, Jan. 2005.

[3] A. Bose and P. Ioannou, "Mixed manual/semi-automated traffic: A macroscopic analysis," *Transport. Res. Pt. C*, vol. 11, pp. 439–462, 2003.

[4] G. Marsden, M. McDonald, and M. Brackstone, "Towards an understanding of adaptive cruise control," *Transport. Res. Pt. C*, pp. 33–51, 2001.

[5] F. Lattemann, K. Neiss, S. Terwen, and T. Connolly, "The predictive cruise control—A system to reduce fuel consumption of heavy duty trucks," SAE International, Warrendale, PA, 2004-01-2616.

[6] J. Zhang and P. Ioannou, "Longitudinal control of heavy trucks in mixed traffic: Environmental and fuel economy considerations," *IEEE Trans. Intel. Transport. Syst.*, vol. 7, no. 1, pp. 92–104, Jan. 2006.

[7] J. Jonsson, "Fuel optimized predictive following in lower speed conditions," M.S. thesis, Dept. Elect. Eng., Linköping Univ., Linköping, Sweden, 2003.

[8] P. Ioannou and Z. Xu, "Throttle and brake control systems for automatic vehicle following," *IVHS J.*, vol. 1, no. 4, pp. 345–377, 1994.

[9] K. Yi and Y. Kwon, "Vehicle-to-vehicle distance and speed control using an electronic-vacuum booster," JASE Rev. vol. 4, pp. 403–412, 2001.

[10] M. Persson, F. Botling, E. Hesslow, and R. Johansson, "Stop and go controller for adaptive cruise control," in *Proc. IEEE Int. Conf. Control Appl.*, 1999, pp. 1692–1697.

[11] A. Higashimata, K. Adachi, T. Hashizume, and S. Tange, "Design of a headway distance control system for ACC," *J. JSAE Rev.*, vol. 22, pp. 15–22, 2001.

[12] D. Corona, M. Lazar, B. Schutter, and M. Heemels, "A hybrid MPC approach to the design of a smart adaptive cruise controller," in *Proc. IEEE Int. Conf. Control Appl.*, Germany, 2006, pp. 231–235.

[13] D. Corona and B. Schutter, "Adaptive cruise control for a SMART car: A comparison benchmark for MPC-PWA control methods," *IEEE Trans. Control Syst. Technol.*, vol. 16, no. 2, pp. 365–372, Mar. 2008.

[14] N. Kohut, F. Borrelli, K. Hedrick, A. Lamprecht, J. Lee, C. Lee, and D. Rosario, "Utilization of intelligent transport systems information to increase fuel economy through engine control," presented at the ITS, New York, 2008.

[15] V. Bageshwar, W. Garrard, and R. Rajamani, "Model predictive control of transitional maneuvers for adaptive cruise control vehicles," *IEEE Trans. Veh. Technol.*, vol. 53, no. 5, pp. 365–374, Sep. 2004.

[16] R. Rajamani, *Vehicle Dynamics and Control*. New York: Springer Verlag, 2005.

[17] C. Fang and D. Xiao, *Process Identification*. China: Tsinghua University Press, 1988.

[18] M. Brackstone and M. McDonald, "Car-following: a historical review," *Transport. Res. Pt. F*, vol. 2, pp. 181–196, 1999.

[19] E. Boer, W. Nicholas, M. Michael, and K. Nobuyuki, "Driver-model-based assessment of behavioral adaptation," presented at the JSAE Spring, Yokohama, Japan, 2005.

[20] L. Zhang, "Driver longitudinal behavior based forward collision warning system," M.S. thesis, Dept. Automot. Eng., Tsinghua Univ., Tsinghua, China, 2006.

[21] K. Xie, L. Han, and J. Dong, *Optimization Method*. Tianjing: Tianjing Univ. Press, 1997.

[22] J. Maciejowski, *Predictive Control With Constraints*. England: Pearson Education, 2002.

[23] S. Li, "Vehicular multi-objective coordinated adaptive cruise control," Ph.D. dissertation, Dept. Automot. Eng., Tsinghua Univ., Tsinghua, China, 2009.

Keqiang Li received the M.S. and Ph.D. degrees from Chongqing University, Chongqing, China, in 1988 and 1995, respectively, and the B.Tech. degree from Tsinghua University, Tsinghua, China, in 1985.

He is currently a Professor with the Department of Automotive Engineering, Tsinghua University. His main areas of research interest include vehicle dynamics and control for driver assistance systems and hybrid electrical vehicles. He has authored over 90 papers and is a coinventor on 12 patents in China and Japan.

Dr. Li has served as a senior member of the Society of Automotive Engineers of China, and on the editorial boards of the International Journal of ITS Research and the International Journal of Vehicle Autonomous Systems. He was a recipient of the "Changjiang Scholar Program Professor" title, and several other awards from public agencies and academic institutions of China.

Rajesh Rajamani received the M.S. and Ph.D. degrees from the University of California at Berkeley, Berkeley, in 1991 and 1993, respectively, and the B.Tech. degree from the Indian Institute of Technology, Madras, India, in 1989.

He is currently a Professor with the Department of Mechanical Engineering, University of Minnesota, Minneapolis. His active research interests include sensors and control systems for automotive and biomedical applications. He has authored over 75 journal papers and is a coinventor on 7 patent applications. He is the author of *Vehicle Dynamics and Control* (Springer Verlag, 2005).

Dr. Rajamani has served as a Chair of the IEEE Technical Committee on Automotive Control and on the editorial boards of the IEEE TRANSACTIONS ON CONTROL SYSTEMS TECHNOLOGY and the IEEE/ASME TRANSACTIONS ON MECHATRONICS. He was a recipient of the CAREER Award from the National Science Foundation, the 2001 Outstanding Paper award from the journal *IEEE Transactions on Control Systems Technology*, the Ralph Teetor Award from SAE, and the 2007 O. Hugo Schuck Award from the American Automatic Control Council.

Shengbo Li received the M.S. and Ph.D. degrees from Tsinghua University, Tsinghua, China, in 2006 and 2009, respectively, and the B.Eng. degree from the University of Science and Technology, Beijing, China, in 2004.

He is currently a Research Fellow with the University of Michigan, Ann Arbor. His active research interests include vehicle dynamics and control, driver behavior, and human factors. He has coauthored over ten journal and conference papers and is a coinventor on six patent applications.

Jianqiang Wang received the B.Tech., M.S., and Ph.D. degrees from Jilin University of Technology, Jilin, China, in 1994, 1997, and 2002, respectively.

He is currently an Associate Professor with the Department of Automotive Engineering, Tsinghua University, Tsinghua, China. His active research interests include intelligent vehicles, driving assistance systems and driver behavior. He has authored over 40 journal papers and is a coinventor on 20 patent applications.

Dr. Wang has engaged in over ten sponsored projects and has received six awards including the "Jilin Province S&T Progress Award" and the "Chinese Automotive Industry S&T Progress Award."